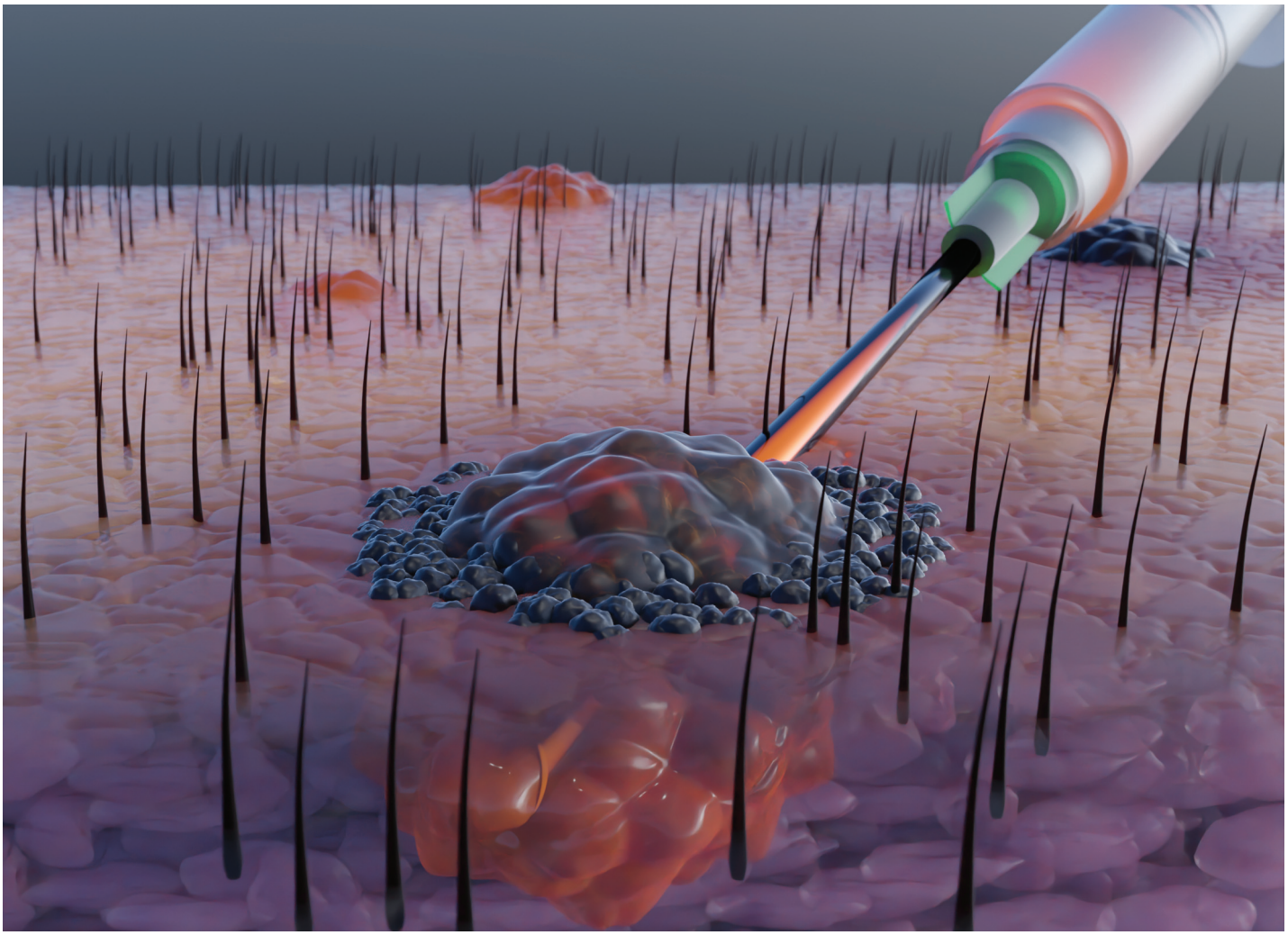

Showcasing research from Prof. Ali Khademhosseini and Prof. Han-Jun Kim's laboratories, Terasaki Institute for Biomedical Innovation (TIBI), Los Angeles, United States.

pH-Responsive doxorubicin delivery using shear-thinning biomaterials for localized melanoma treatment

This study demonstrates that doxorubicin-loaded gelatin/LAPONITE®-based shear-thinning biomaterials (STBs) exhibit pH-responsiveness and highly controlled and sustained release of therapeutic drugs for injectable anti-tumoral applications. In particular, it highlights the importance of tailored engineering of STBs by controlling their compositions of gelatin/LAPONITE®.

As featured in:

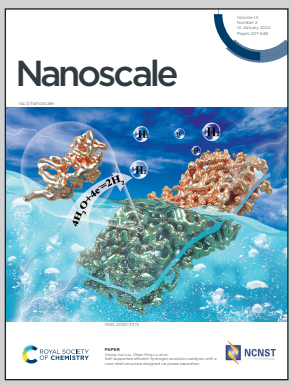

See Ali Khademhosseini, Han-Jun Kim *et al.*, *Nanoscale*, 2022, **14**, 350.

ROYAL SOCIETY OF CHEMISTRY

rsc.li/nanoscale

Registered charity number: 207890

Nanoscale

PAPER

View Article Online
View Journal | View Issue

Cite this: *Nanoscale*, 2022, **14**, 350

pH-Responsive doxorubicin delivery using shear-thinning biomaterials for localized melanoma treatment†

Junmin Lee,[a,b,c,d] Yonggang Wang,[c,d,e] Chengbin Xue,[c,d,f,g] Yi Chen,[c,d,h] Moyuan Qu,[c,d] Jai Thakor,[c,d] Xingwu Zhou,[c,d] Natan Roberto Barros,[a] Natashya Falcone,[a] Patric Young,[a] Floor W. van den Dolder,[c,d] KangJu Lee,[a,c,d,i] Yangzhi Zhu,[a] Hyun-Jong Cho,[c,d,j] Wujin Sun,[a,c,d] Bo Zhao,[h] Samad Ahadian,[a,c,d] Vadim Jucaud,[a] Mehmet R. Dokmeci,[a,c,d] Ali Khademhosseini *[a,c,d] and Han-Jun Kim *[a,c,d]

Injectable shear-thinning biomaterials (STBs) have attracted significant attention because of their efficient and localized delivery of cells as well as various molecules ranging from growth factors to drugs. Recently, electrostatic interaction-based STBs, including gelatin/LAPONITE® nanocomposites, have been developed through a simple assembly process and show outstanding shear-thinning properties and injectability. However, the ability of different compositions of gelatin and LAPONITE® to modulate doxorubicin (DOX) delivery at different pH values to enhance the effectiveness of topical skin cancer treatment is still unclear. Here, we fabricated injectable STBs using gelatin and LAPONITE® to investigate the influence of LAPONITE®/gelatin ratio on mechanical characteristics, capacity for DOX release in response to different pH values, and cytotoxicity toward malignant melanoma. The release profile analysis of various compositions of DOX-loaded STBs under different pH conditions revealed that lower amounts of LAPONITE® (6NC25) led to higher pH-responsiveness capable of achieving a localized, controlled, and sustained release of DOX in an acidic tumor microenvironment. Moreover, we showed that 6NC25 had a lower storage modulus and required lower injection forces compared to those with higher LAPONITE® ratios. Furthermore, DOX delivery analysis *in vitro* and *in vivo* demonstrated that DOX-loaded 6NC25 could efficiently target subcutaneous malignant tumors *via* DOX-induced cell death and growth restriction.

Received 31st August 2021,
Accepted 3rd November 2021

DOI: 10.1039/d1nr05738c

rsc.li/nanoscale

1. Introduction

Shear-thinning biomaterials (STBs) have unique mechanical characteristics such that their viscosity decreases under shear stress and their modulus can be restored to its initial value after injection.[1] These unique mechanical characteristics enable the administration of therapeutic agents locally to a target site through thin needles and catheters, and are particularly useful for targeting localized cancer,[2] embolization,[3] injuries,[4] and inflammation.[5] In addition, compared to the conventional chemotherapies administered in single doses which circulate throughout the body, STBs allow for targeted and sus-

[a]*Terasaki Institute for Biomedical Innovation, Los Angeles, CA 90064, USA. E-mail: khademh@terasaki.org, hkim@terasaki.org*
[b]*Department of Materials Science and Engineering, Pohang University of Science and Technology (POSTECH), Pohang 790-784, Korea*
[c]*Department of Bioengineering, Henry Samueli School of Engineering and Applied Sciences, University of California, Los Angeles, Los Angeles, CA 90095, USA*
[d]*Center for Minimally Invasive Therapeutics, University of California, Los Angeles, Los Angeles, CA 90095, USA*
[e]*Guangdong Engineering & Technology Research Center for Quality and Efficacy Reevaluation of Post-Market Traditional Chinese Medicine, Guangdong Key Laboratory of Plant Resources, School of Life Sciences, Sun Yat-sen University, Guangzhou 510275, P. R. China*
[f]*Key Laboratory of Neuroregeneration, Ministry of Education and Jiangsu Province, Co-innovation Center of Neuroregeneration, Nantong University, Nantong, Jiangsu, 226001, P.R. China*
[g]*Jiangsu Clinical Medicine Center of Tissue Engineering and Nerve Injury Repair, Research Center of Clinical Medicine, Affiliated Hospital of Nantong University, Nantong, Jiangsu 226001, P.R. China*
[h]*Department of Research and Design, Beijing Biosis Healing Biological Technology Co., Ltd, Daxing District, Biomedical Base, Beijing 102600, P. R. China*
[i]*Department of Healthcare and Biomedical Engineering, Chonnam National University, Yeosu 59626, Republic of Korea*
[j]*College of Pharmacy, Kangwon National University, Chuncheon, Gangwon 24341, Republic of Korea*

†Electronic supplementary information (ESI) available. See DOI: 10.1039/d1nr05738c

tained delivery of chemotherapeutics while off-target effects are minimized.[6] STBs can be crosslinked through various mechanisms, including physical crosslinking (*e.g.*, ionic interactions and aggregation approaches) and self-assembly (*e.g.*, host–guest, hydrogen bonds, and electrostatic interactions).[7] Among the various STBs with these different mechanisms, nanocomposite hydrogels based on electrostatic interactions have been employed due to their simple assembly and outstanding shear-thinning properties and injectability.[2,8,9] For example, gelatin (bearing both positive and negative charges with primary amines and carboxylic acids, respectively)-LAPONITE® nanoclay (bearing both negative and positive charges at the surface and rim, respectively) mixtures with strong electrostatic attraction simply formed physically crosslinked hydrogels.[10] In addition, it was also shown that different types and concentrations of ions could affect shear-thinning properties and injectability of gelatin-LAPONITE® hydrogels.[9]

The microenvironment of malignant tumors is known to be acidic (~pH 5.6–6.8).[11–13] For this reason, lots of studies have been performed to provide sustained, localized molecule/drug delivery using pH-responsive biomaterials.[14] For instance, LAPONITE® previously showed a pH-dependent release of doxorubicin (DOX) on target tumors.[15] In the study, DOX could be loaded onto the surface of LAPONITE® through electrostatic interactions, and the loaded DOX was released in a pH-dependent manner. The loading/releasing of DOX in LAPONITE®-based systems may be controlled by (i) electrostatic attraction/repulsion between DOX and LAPONITE®, (ii) hydrogen bonding, (iii), intercalation/withdrawal of DOX from LAPONITE®s, and (iv) ionic exchange between them.[16] In addition, skin cancer has been targeted using curcumin, DOX, or 5-fluorouracil loaded nanogels to release such molecules/drugs specifically to the site of action at appropriate concentrations/times.[17–23] Although these nanogel-based systems could provide localized release of loaded molecules/drugs to target melanoma, shear-thinning properties were not obtained. Compared with nanogel-based targeting of melanoma, STB-based drug delivery provides (1) long-term *in vitro* and *in vivo* stability without fragmentation or nontarget embolization, (2) rapid delivery through clinical catheters and needles, and (3) versatility to target other cancer types in the body. Importantly, nanogels could be engineered to have shear-thinning properties to enhance the performance and efficacy to target tumors. Previously, we have employed gelatin/LAPONITE® STBs to investigate the role of compositions in the variation of mechanical/bioactive properties,[2] their clinical applicability especially for hemostasis and endovascular embolization,[3,4] and the ionic effects on their injectability and rheological properties.[9] However, it is still unclear how different compositions of gelatin and LAPONITE® could regulate DOX release at different pH values to enhance the effectiveness of localized skin cancer treatment. Therefore, we reasoned that comparing gelatin/LAPONITE® STBs with their different compositions will provide insight into efficiently targeting subcutaneous malignant tumors. To this end, we employed STBs with different LAPONITE®/gelatin ratios (gelatin 4.5%/LAPONITE® 1.5%: 6NC25, gelatin 3.0%/LAPONITE® 3.0%: 6NC50, and gelatin 1.5%/LAPONITE® 4.5%: 6NC75, total 6% (w/v)) as a vehicle for sustained and localized drug delivery, so that their composition differentially influence their mechanical properties, DOX release capacity for different pH values, and cytotoxicity/growth restriction toward malignant melanoma. STBs were not applied topically, but were injected directly into the tumor.

2. Materials and methods

2.1 STB preparation

Porcine skin gelatin (18% (w/v); G1890, Sigma, CA, USA) and silicate nanoplatelets (9% (w/v); LAPONITE® XLG, BYK) were mixed in Milli-Q de-ionized (DI) water to prepare a stock solution. The gelatin solution was heated at 80 °C for a minimum of 30 min for full dissolution. At the same time, LAPONITE® was mixed using a SpeedMixer at 2500 rpm for 5 min until particles were completely dissolved. STB formulations were prepared by mixing specified quantities of LAPONITE® and gelatin (for 6NC25: 0.045 g mL^{-1} of gelatin and 0.015 g mL^{-1} of LAPONITE®, for 6NC50: 0.030 g mL^{-1} of gelatin and 0.030 g mL^{-1} of LAPONITE®, and for 6NC75: 0.015 g mL^{-1} of gelatin and 0.045 g mL^{-1} of LAPONITE®). The mixtures were spun in the SpeedMixer until the solutions were fully dispersed.

2.2 Rheological evaluation

The rheological properties of shear stress/viscosity/storage moduli of the STBs were assessed using parallel plate geometry on an Anton Paar rheometer (AR-G2, TA instruments protocol). Once samples were loaded onto the plate, mineral oil was added around the plate to prevent any evaporation of the hydrogel samples during the run. To complete an oscillatory stress sweep, 0.1–1000 Pa under a fixed oscillatory frequency of 1 Hz were applied. To achieve an oscillatory frequency sweep, 0.1–100 Hz under a fixed oscillatory stress of 10 Pa at 25 °C were applied. The recorded shear stress/viscosity/storage moduli values were analyzed using the Anton Paar Rheocompass™ software.

2.3 Loading of DOX within STBs

The STBs were mixed thoroughly with different quantities of an aqueous DOX solution (Oakwood Chemical, SC, USA) of 10 mg mL^{-1} with a spatula, and then placed in a SpeedMixer to evenly distribute the components to obtain final concentrations of 1, 10, 100, and 1000 μg g^{-1}.

2.4 DOX release study *in vitro*

The DOX-STB mixture was investigated by the dialysis of DOX-STB against acidic Dulbecco's phosphate buffered saline (DPBS; pH 6.5, Gibco, CA, USA). The STBs were immersed in a semi-permeable dialysis membrane within DPBS of predetermined pH levels (5.0, 6.0, or 7.4) and measured at specific time intervals to determine the concentrations of DOX follow-

ing release. To quantify DOX diffusion into the surrounding DPBS, the solution was continuously re-weighed for up to 30 days on a weighing scale. Interference between LAPONITE® and gelatin for DOX quantification was not observed, and the polycarbonate membrane had a pH resistance within the range of pH used in the study.

2.5 DOX-STB cytotoxicity assessment *in vitro*

The B16F10 murine melanoma cell line was obtained from American Type Culture Collection (ATCC, Manassas, VA, USA) and maintained in Dulbecco's Modified Eagle Medium (DMEM; Gibco, CA, USA) supplemented with 10% fetal bovine serum (FBS; Gibco, CA, USA), 50 μg mL^{-1} streptomycin, and a 50 U mL^{-1} penicillin (Pen/Strep; Gibco, CA, USA) solution. Following culture, the cells were incubated at 37 °C under a 5% CO_2 atmosphere. The cells were passaged using trypsin EDTA (Gibco, CA, USA) at 80–90% confluency and seeded into 24-well Transwell plates (Corning, USA) and a 24-well plate (Corning, USA) at 5×10^4 cells per well. After one day of incubation at 37 °C and 5% CO_2, the STBs were added to the insert of the Transwell plate or into the well directly above the cells, and the media were replaced. After incubation for 1, 3, or 7 days, cell viability was examined using a Live/Dead viability/cytotoxicity kit (Invitrogen, USA). A fluorescence microscope (Zeiss Axio Observer; Carl Zeiss, Jena, Germany) was employed for imaging. Ten non-overlapping areas (200× magnification) were employed for quantitative data analysis using the Image J software (NIH, MD, USA). The viability of cells (%) was calculated as the ratio of the living cell number to the total cell number.

2.6 Anti-tumor efficacy evaluation *in vivo*

Six-week-old female C57Bl/6J mice were obtained from Jackson Laboratories (Bar Harbor, ME, USA). The UCLA Animal Research Committee (UCLA ARC #2019-044-01A) approved all animal studies. General inhalation anesthesia with isoflurane (5% for induction and 2–3% for maintenance and 2 L min^{-1} oxygen flow as indicated) was induced and maintained by spontaneous inhalation through a face mask. The injection site was shaved and disinfected before tumor cell injection. B16F10 cells (1×10^6 in 100 μl of DPBS diluted Matrigel [1 : 1]) were injected subcutaneously into the flank. When the tumor volumes reached around 50–100 mm^3, 50 μL of experimental materials were injected into the tumor. The negative control group was injected with DPBS. Blank STBs (6NC25 and 6NC75), DOX (5 mg kg^{-1}), and DOX-loaded STBs (DOX-6NC25 and 6NC75; 5 mg kg^{-1} of DOX) were injected into the tumor. For the survival test, six mice of each group were tested to evaluate the survival rate during the experimental period. The experimental endpoint was defined as either a humane endpoint or a tumor size greater than 2000 mm^3 or >15 mm in diameter. For the tumor size growth analysis, the tumor size was measured every two days using a caliper. Six mice of each experimental group were euthanized (CO_2 inhalation) post-operation day 10. Tissue samples (the tumor, liver, lungs, heart, spleen, and kidneys) were obtained and fixed in 10% neutralized buffered formalin (Leica Biosystems, IL, USA), and then histological analysis was performed.

2.7 Histopathological evaluation

Formalin-fixed tissue samples were subjected to the standard paraffin-based histological evaluation (dehydration, clearing, xylene processing, and embedding). Routine hematoxylin (Leica Biosystems) and eosin (Sigma) (H&E) staining was employed for the staining of 4 μm thick tissue sections. A Zeiss inverted microscope was used to image the histology samples. For quantitative analysis (tumor area and the amount of cells/positivity of immunofluorescence), Image J (NIH, MD, USA) and AmScope (Irvine, CA, USA) image analysis software were used. For immunostaining, the sections were deparaffinized, antigen retrieved (citrate-buffered and heat-induced), and permeabilized in PBST (0.3% Triton in DPBS), followed by incubation with bovine serum albumin for 30 min. The primary antibodies used were the anti-Ki67 rabbit polyclonal antibody (Abcam, CA, USA), anti-caspase-3 antibody (Novus Biologicals, CO, USA), and BrdU-Red TUNEL assay kit. A goat anti-mouse IgG Alexa Fluor 488 conjugated antibody (ThermoFisher) and goat anti-rabbit IgG Alexa Fluor 594 conjugated antibody (ThermoFisher) were used as secondary antibodies. The sections were counterstained with DAPI using a fluoromount (Vector Laboratories, CA, USA). Fluorescence images were obtained using an inverted fluorescence microscope (Axio Observer 5, Zeiss, Germany).

2.8 Statistical analysis

Mean ± standard deviation was used for presenting all data. More than a triplicate of group data sets were used for analyzing statistics; multiple comparisons were performed using one-way ANOVA with Bonferroni *post hoc* tests. $p < 0.05$ was assumed to be statistically significant.

3. Results and discussion

3.1 STBs for sustained and pH-responsive release of DOX

Stimuli-responsive biomaterials have shown the potential to enhance the delivery of therapeutics to tumor cells in a controlled and sustained manner.[14] To specifically target an acidic tumor microenvironment, we employed pH-responsive gelatin/LAPONITE®-based STBs, and gelatin and LAPONITE® were used as controls. LAPONITE® has previously been shown to release DOX in a pH-dependent manner: the DOX release increased as the pH decreased.[15] In addition, gelatin is a polyampholyte of which electrical charge is affected by pH fluctuations.[24] Hence, we first hypothesized that the DOX release profiles from the STBs could be affected by different mixing ratios between gelatin and LAPONITE®. Therefore, the DOX in gelatin/LAPONITE®-based STBs could be released due to ion-exchange interactions at different pH values,[25] and thus it is strongly required to determine the optimum gelatin/LAPONITE® mixing ratio to maximize therapeutic

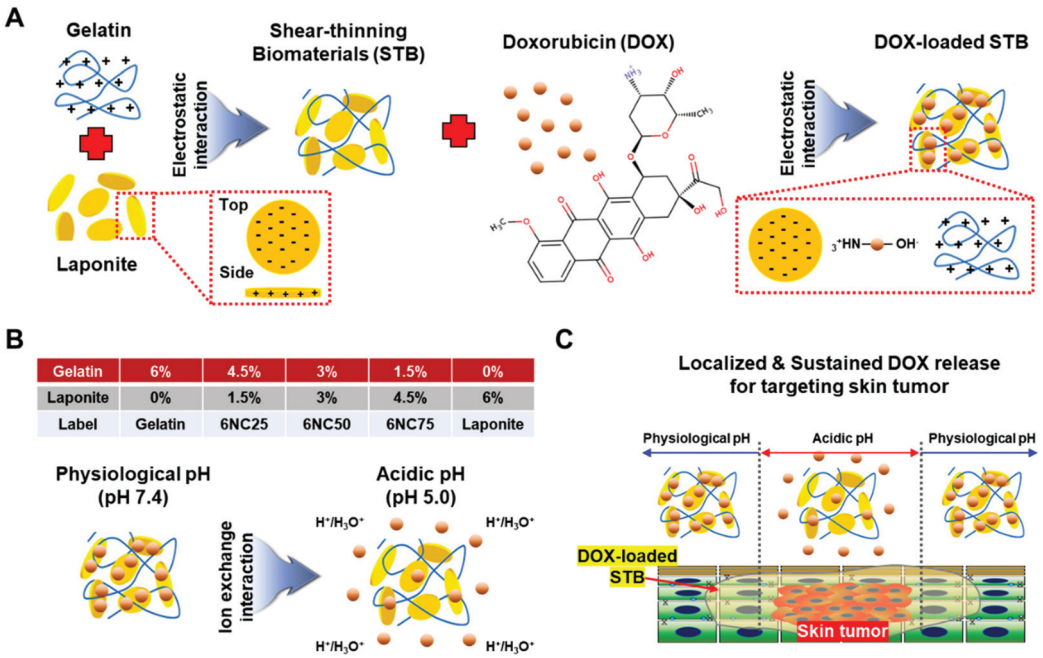

Gelatin	6%	4.5%	3%	1.5%	0%
Laponite	0%	1.5%	3%	4.5%	6%
Label	Gelatin	6NC25	6NC50	6NC75	Laponite

Fig. 1 pH-Responsive DOX delivery using STBs for localized melanoma treatment. (A) Schematic exhibiting DOX-containing, gelatin/LAPONITE®-based STB fabrication. (B) Table with composition information for biomaterials with different ratios between gelatin and LAPONITE® and proposed pH-responsive delivery of DOX-STBs. (C) Schematic displaying pH-responsive DOX delivery using STBs for localized melanoma treatment.

efficacy (Fig. 1). As expected, the DOX release from gelatin/LAPONITE®-based STBs was pH-dependent, with a greater release in the more acidic environment for 30 days (Fig. 2A and S1†). Gelatin showed a dramatic increase in DOX release within the first 3 days—the highest release profile at approximately 75–90% regardless of pH variations—and then a gradual increase over the experimental periods (Fig. 2B–D). However, the STBs and LAPONITE® only maintained release profiles below 10% at pH 7.4, indicating that LAPONITE® dampens the DOX release properties of gelatin at a physiological pH (Fig. 2B). At pH 6.0, 6NC25 was the only STB condition showing DOX release profiles slightly above 30% while the others still showed release profiles below 10% (Fig. 2C). This suggests that the STBs with lower LAPONITE® (6NC25) could sustain a greater release profile at pH 6.0 compared to the other STBs with higher LAPONITE® (6NC50 and 6NC75). At pH 5.0, all STB conditions and the LAPONITE® only control exhibited higher release profiles compared to those at pH 7.4 and pH 6.0 (Fig. 2D). At pH 5.0, 6NC25 had the second greatest release profile at ~55%, followed by 6NC50 (~40%), 6NC75 (~40%), and LAPONITE® alone (~20%). To investigate the pH-responsiveness of the DOX release, the release rates of DOX at pH 5.0 were subtracted from the release rates at pH 7.4 (Fig. 2E and F). We noticed that 6NC25 showed a higher pH-responsiveness of DOX release above ~50% than 6NC50 (~30%), 6NC75 (~30%), gelatin (~5%) and LAPONITE® alone (~20%) after 12 days. These findings suggest that 6NC25 may prove to be important for the controlled and sustained release of DOX locally under acidic conditions.

3.2 Mechanical properties of DOX-STBs and their injectability *via* different syringe and needle sizes

Syringes and catheters are typically used to deliver therapeutic agents to target sites, so the STBs need to be easy to administer and maintain their properties during injection. We injected gelatin/LAPONITE® STBs at various injection conditions (a 1cc syringe or 3cc syringe with different sizes of needles, 18G, 23G, and 25G) with or without DOX (Fig. 3A and B). Concerning the rheological properties of the STBs, first, we measured the storage modulus to verify the recovery of the STBs after deformation (Fig. 3C). In general, STBs can recover when exposed to shear stress, which indicates their strength following injection into the applied site, regardless of the amount of DOX loaded into the STBs. In addition, it was observed that 6NC25 showed the lower storage capacity and the lowest strain at the low and high strain levels. The swelling and degradation profiles of the STBs have been previously studied.[2] To determine the stability of the STBs 6NC25, 6NC50, and 6NC75 compositions over time, the STBs were exposed to time changes in shear strain *versus* modulus and their viscosity properties were quantified (Fig. 3D). 6NC25 exhibited the fastest recovery among the three compositions. In addition, 6NC25 displayed lower viscosity degrees compared to 6NC75, meaning a lower resistance to mechanical deformation and flow. This indicates that their shear-thinning properties increase with increasing gelatin and decreasing LAPONITE® concentrations. We then measured the force, which showed a linear increase until it plateaued at the material's injection force (Fig. S2†). The STBs exhibited distinct levels of injection forces at various syringe sizes

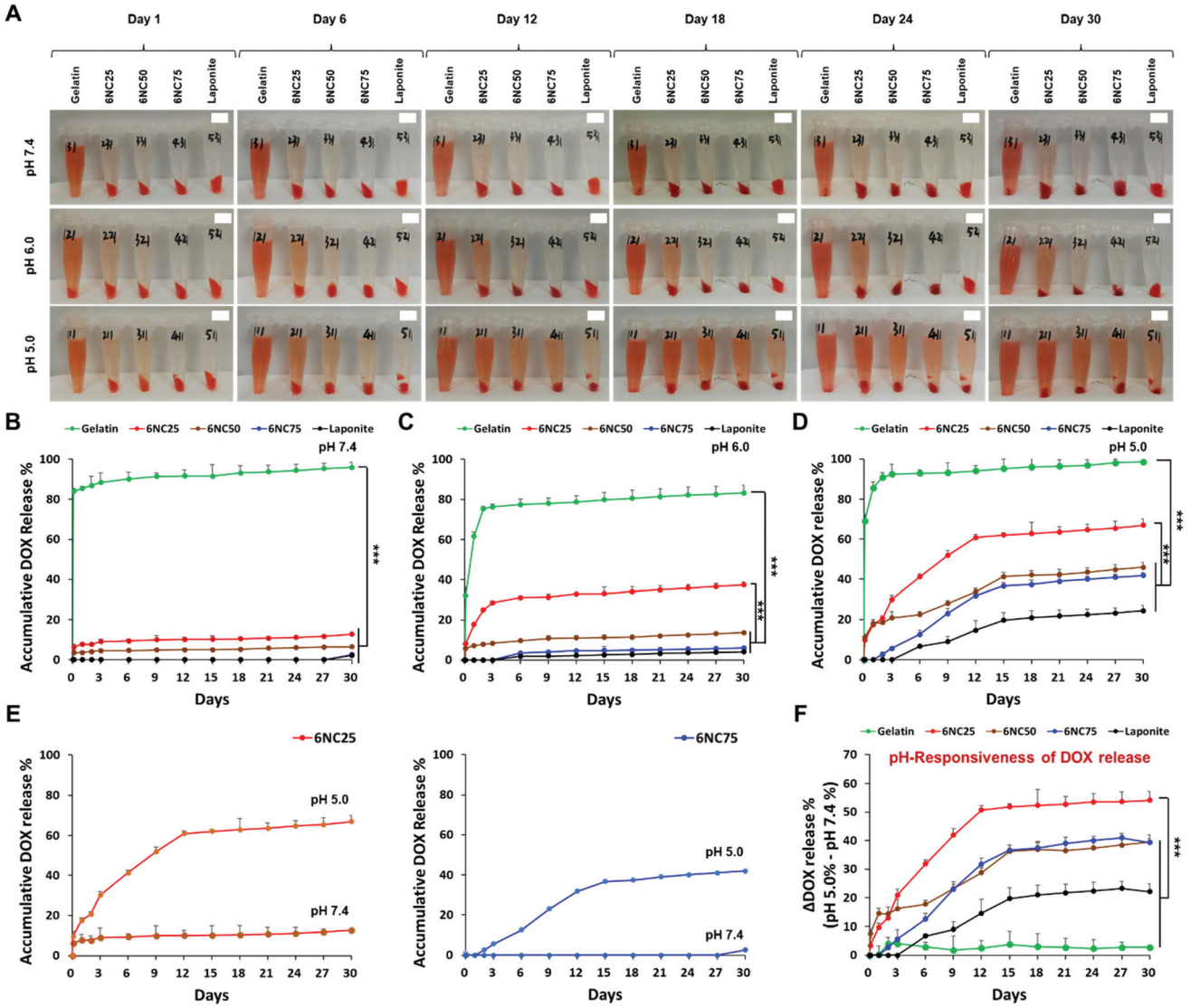

Fig. 2 STBs allowing for the sustained and pH-responsive release of DOX. (A) Representative images of biomaterials with different compositions between gelatin and LAPONITE® showing DOX release (100 μg mL^{-1}, red color) at pH 7.4, 6.0, and 5.0 for 30 days. Red palette in solution: aggregation of STB containing DOX. Red solution: released DOX from DOX. Release profiles of various compositions of DOX-loaded STBs at pH (B) 7.4, (C) 6.0, and (D) 5.0 for 30 days. (E) Accumulative DOX release differences for 6NC25 and 6NC75 at pH 5.0 and 7.4. (F) pH-Responsiveness of DOX release from STBs. The values of DOX release at pH 5.0 were subtracted from those at pH 7.4. Scale bar is 1 cm. ***$p < 0.001$, ANOVA. Error bars are the standard deviation.

(Fig. 3E and F). 6NC25 was observed to require lower injection forces compared to those with higher LAPONITE® ratios. Additionally, the force required to inject STBs increased with increasing syringe volume (injection force using 3cc > injection force using 1cc syringes) as well as needle sizes (25G > 23G > 18G).

3.3 *In vitro* cytotoxicity of DOX-STBs in melanoma

Before evaluating the effectiveness of DOX-STBs for targeting skin cancers *in vivo*, we questioned whether different DOX-STB conditions with different pH-responsive release profiles could affect melanoma cell growth and viability. In addition, if their growth and viability could be regulated by different formulations of DOX-STBs, it is important to find the most effective concentration of DOX. To answer these questions, we employed highly metastatic murine B16F10 melanoma cells for an *in vitro* cytotoxicity test model. First, the cells were seeded onto well plates and a near-monolayer culture was achieved. Next, STBs mixed with DOX with varying concentrations were applied by adding directly onto cells in the culture plate (direct contact, Fig. 4A). We did not include the 6NC50 condition because it showed an intermediate effect between 6NC25 and 6NC75. We observed that the cells cultured in the control group (no STB/DOX treatment) or STB groups (6NC25 and 6NC75) without DOX grew exponentially for 7 days (Fig. 4B). The number of cells per field decreased with increasing DOX concentration. In particular, the cells

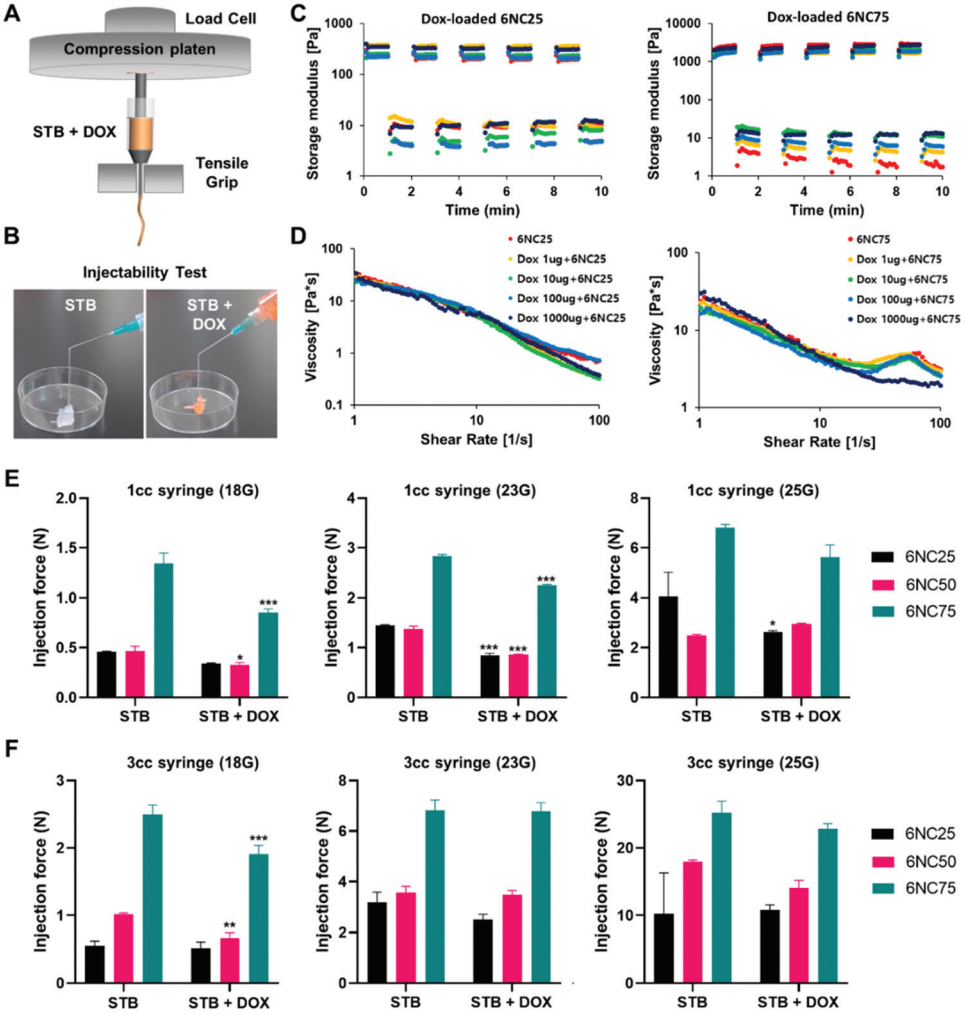

Fig. 3 Rheological properties and injectability of STBs through various syringe and needles sizes. (A) Schematic exhibiting the injection force measurement setup. An Instron mechanical tester was employed to access the injection forces of different STB conditions. (B) Representative images displaying the injectability of STBs with or without DOX through a catheter/syringe. (C) Storage modulus and (D) viscosity of 6NC25 and 6NC75 STBs. Injection forces for different compositions of STBs through (E) a 1cc syringe or (F) 3cc syringe with different sizes of catheters. *; compared to the STBs without DOX. *$p < 0.05$, **$p < 0.01$, ***$p < 0.001$, ANOVA. Error bars are the standard deviation.

treated with DOX-6NC25 (1 μg) showed significantly decreased growth rates compared to cells treated with free DOX or DOX-6NC75 at the same DOX concentrations. These results may indicate that the sustained release of low concentration DOX can effectively reduce the growth rate of melanoma cells compared to one-time free DOX delivery. Moreover, DOX-6NC25 with even higher concentrations of DOX (10–1000 μg) significantly reduced cellular growth rates compared to DOX-6NC75. This result shows that DOX-6NC25 may have a better release profile of DOX in response to the decreased pH seen in the acidic microenvironment of melanoma, consistent with the DOX release profiles of STBs (Fig. 2E). Furthermore, cell viability was measured among visible cells across the conditions (Fig. 4C and D). The viability of cells cultured with DOX-6NC25 (100 μg of DOX) was significantly reduced at day 3 compared to cells treated with free DOX or DOX-6NC75 at the same DOX concentration.

When the cells are in direct contact with DOX-STBs, there may be two possible mechanisms of DOX release: pH-responsive release and cell–STB interaction-associated release. To examine the sole effect of pH-responsive release, the STBs were injected into a Transwell insert of the culture plate (indirect contact, Fig. 5A). Since DOX penetrates through Transwell membranes, it can reach melanoma cells cultured on well plates. We observed that the cells treated with free DOX using the Transwell showed a similar cell number per field compared to the outcome using free DOX *via* direct contact (Fig. 5B). In addition, the cells cultured with DOX-6NC25 (1–100 μg of DOX) on Transwells exhibited significantly decreased cell growth compared to those cultured with DOX-6NC75. These trends also correspond to those from the direct contact with DOX-STBs, even though the addition of DOX-STBs using Transwells resulted in a subtly decreased efficacy of inhibiting melanoma growth. These results indicate that the primary

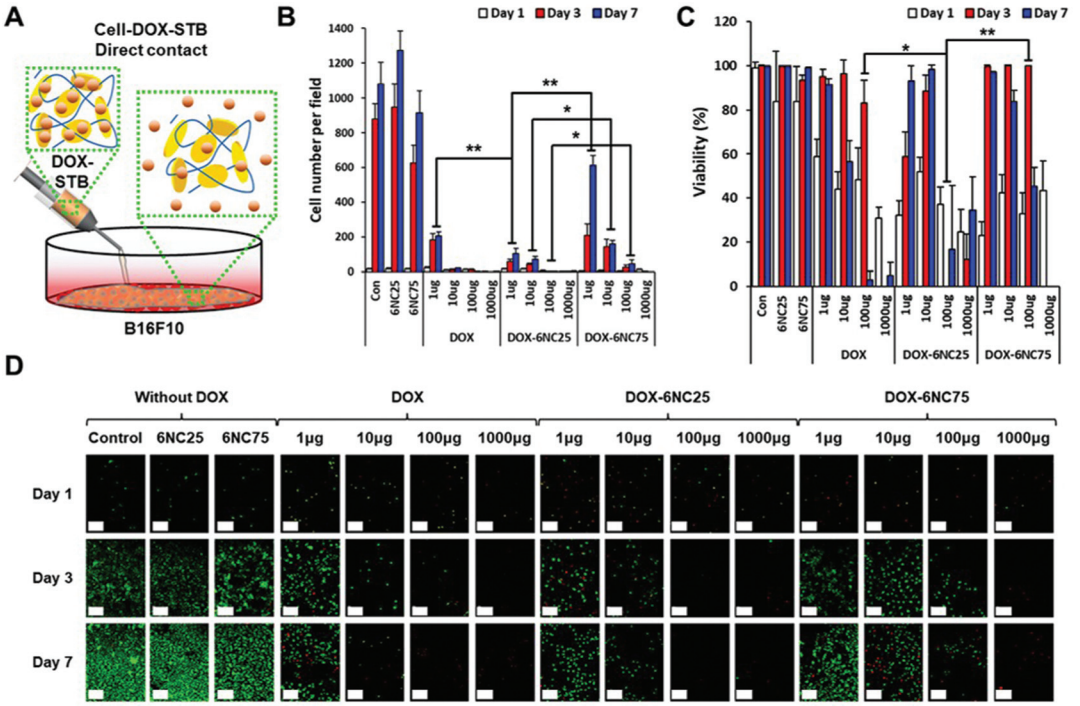

Fig. 4 *In vitro* direct contact cytotoxicity of DOX-STBs in melanoma. (A) Schematic exhibiting direct contact between cells and DOX-STBs. (B) Quantified cell number per field across the samples with different DOX concentrations. (C) Quantified viability and (D) representative live/dead fluorescence images of B16F10 melanoma treated with different conditions for 7 days. Scale bar is 100 μm. *$p < 0.05$, **$p < 0.01$, ANOVA. Error bars are the standard deviation.

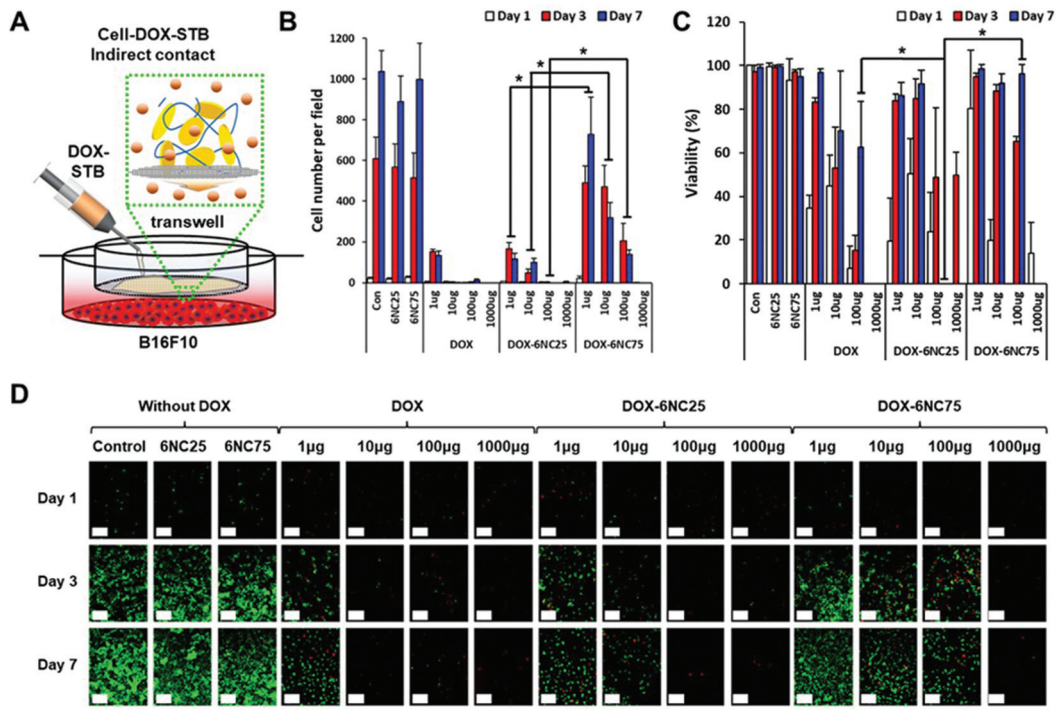

Fig. 5 *In vitro* indirect contact cytotoxicity of DOX-STBs in melanoma. (A) Schematic exhibiting indirect contact between cells and DOX-STBs using a Transwell. (B) Quantified cell number per field across the samples with different DOX concentrations. (C) Quantified viability and (D) representative live/dead fluorescence images of B16F10 melanoma treated with different conditions for 7 days. Scale bar is 100 μm. *$p < 0.05$, ANOVA. Error bars are the standard deviation.

mechanism of DOX release from DOX-STBs could be the pH-responsive release. Furthermore, a similar pattern of cell viability trends was observed in direct and indirect contacts (Fig. 5C and D).

3.4 DOX-STBs targeting skin tumors *in vivo*

We speculated that the localized delivery of DOX-STBs and their pH-responsive DOX release could improve the therapeutic efficacy for metastatic skin cancers. To verify this, we produced a murine skin cancer model by subcutaneous injection of the B16F10 melanoma cell line into 6-week-old female C57BL/6 mice (Fig. 6A). Experimental materials (DOX, STBs, and DOX-STBs) were then injected into the mice intratumorally. To confirm the efficient delivery of DOX from DOX-STBs, the same sample conditions used for *in vitro* direct/indirect cytotoxicity of DOX-STBs in the melanoma study were employed (control: untreated, 6NC25: without DOX, 6NC75: without DOX, free DOX: without STBs, DOX-6NC25: with DOX, and DOX-6NC75: with DOX). According to the Kaplan–Meier survival analysis, the group with DOX (DOX, DOX-6NC25, and DOX-6NC75) survived longer than the group without DOX (tumor, 6NC25, and 6NC75) (Fig. 6B and S3A†). STB injection did not have a positive/negative effect on the survival rate. Interestingly, the mice injected with DOX-6NC25 survived longer than either free DOX or DOX-6NC75, demonstrating the efficacy of DOX-loaded STBs in mice with subcutaneous malignancies. Then, we analyzed the effect of DOX-loaded STBs on tumor growth over time in the B16F10 melanoma model. At the time of treatment (day 0), the tumor sizes of all of the groups were less than 100 mm^3. The tumor growth was inhibited in the DOX-loaded groups (DOX and DOX-STBs) compared to the groups without DOX (tumor and STBs). Similar to survi-

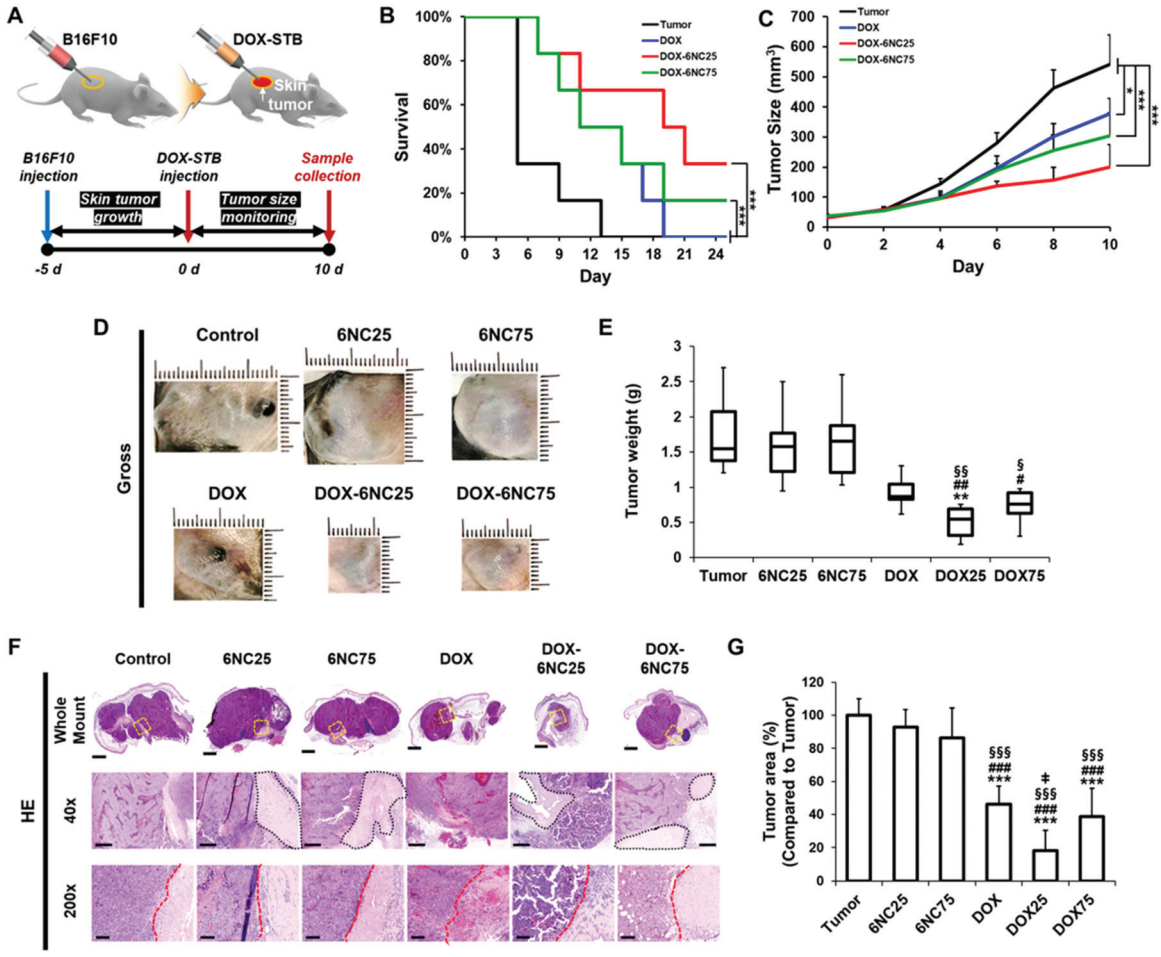

Fig. 6 DOX-STBs targeting skin tumors *in vivo*. (A) The timeline for the *in vivo* experiments. (B) Kaplan–Meier analysis of C57BL/6 mice after subcutaneous injection of STBs. (C) Tumor growth curve for the melanoma-bearing mice injected with DOX-loaded STBs. *$p < 0.05$, **$p < 0.01$, ***$p < 0.001$, ANOVA. (D) Representative images showing *in vivo* anti-melanoma cancer efficacy of DOX-STBs. (E) Quantification of tumor weights after 8 days of injections of DOX-STBs. *; compared to the tumor, #; compared to 6NC25, and §; compared to 6NC75. *$p < 0.05$, **$p < 0.01$, ***$p < 0.001$, ANOVA. (F) Histopathology of tumor sections treated with different conditions. Black dotted line: STBs remnant, red dotted line: the tumor border (left; tumor and right; STBs or hemorrhage/necrotic lesion). Scale bar is 2 mm, 500 μm, and 100 μm for whole mount, 40×, and 200×, respectively. Error bars are the standard deviation. (G) Quantitative tumor area analysis. *; compared to the tumor, #; compared to 6NC25, §; compared to 6NC75, and ‡; compared to DOX. *$p < 0.05$, **$p < 0.01$, ***$p < 0.001$, ANOVA.

val analysis, the treatment with DOX-6NC25 led to significantly smaller tumors for 10 days compared to the other conditions (Fig. 6C, D and S3B†). The DOX-6NC25 group significantly inhibited tumor growth compared to the other DOX-loaded groups, which were 48% and 34% smaller than the DOX and DOX-6NC75 groups, respectively. As a result of the analysis of the tumor weights collected after sacrifice, the median tumor weight of the DOX-6NC25 group was significantly smaller than that of the tumors treated without DOX, and it was smaller than that of the free DOX or DOX-6NC75 groups (Fig. 6E). Further histopathological evaluation was performed on subcutaneous tumors to analyze the percentage of tumor surface area and necrotic lesions across conditions (Fig. 6F). As a result of H&E staining, STBs injected into the tumor (with/without DOX) were not degraded in 10 days and remained around the tumor (Fig. 6F, black dotted line). In the case of DOX-6NC25, we assumed that the DOX-loaded STBs would appear to cover the tumor, resulting in a wide range of inflammatory/necrotic reactions, whereas, in the DOX-6NC75 group, it would appear to be displaced contralateral to the tumor, although further demonstration will be required. In particular, cell death/necrosis and inflammatory cell infiltration were prominent upon contact with DOX-STBs (Fig. 6F, red dotted line). Quantitative analysis of the tumor area revealed that malignant melanoma treated with DOX-6NC25 showed the lowest tumor area compared with STBs only, free DOX, and DOX-6NC75. These results are consistent with the results of the Kaplan–Meier survival analysis as well as tumor volume and mass measurements (Fig. 6G).

Finally, we analyzed the changes in apoptosis (caspase-3, TUNEL) and proliferation (Ki67) markers in DOX-STB applied tumor samples (Fig. 7 and Fig. S5†). As shown in Fig. 7, higher caspase-3 expression and lower Ki67 expression were noted in the DOX-treated groups (DOX and DOX-STBs) compared to the non-DOX-treated groups (tumor and STBs). In addition, an increase in apoptotic cell death was clearly observed in the DOX-treated groups on TUNEL staining (Fig. S5†). Among these DOX-treated groups, DOX-6NC25 showed a statistically significant decrease in proliferation markers and an increase in tumor cell death markers. As a result of this study, DOX-6NC25 showed a superior antitumor effect than free DOX or DOX-6NC75. These results can be attributed to the difference in the release profile and tumor penetrability according to the composition of DOX-STBs. In our results (Fig. 2 and S1†), all DOX-STBs showed a pH-responsive DOX-release profile. However, it was confirmed that DOX release was faster

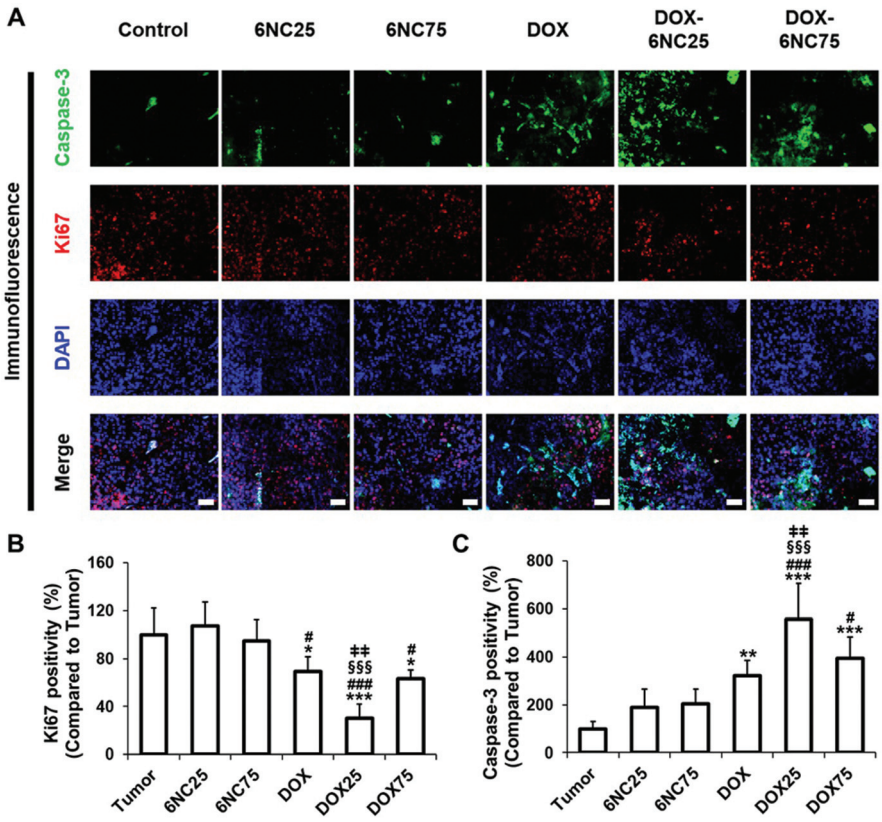

Fig. 7 Apoptosis and proliferation analysis for tumor samples treated with DOX-STBs. (A) Representative immunofluorescence images of excised tumor tissues stained with DAPI (blue), Ki67 (red), and caspase-3 (green) under different conditions. The average percentage of cells positively expressing (B) Ki67 and (C) caspase-3. Scale bar is 50 μm. *; compared to the tumor, #; compared to 6NC25, §; compared to 6NC75, and ‡; compared to DOX. *$p < 0.05$, **$p < 0.01$, ***$p < 0.001$, ANOVA. Error bars are the standard deviation.

as the amount of LAPONITE® decreased. In addition, as the ratio of LAPONITE® increases, mechanical stability increases, resulting in a tendency to stay at the injection site rather than spread around the tumor. That is, in a rapidly growing skin tumor such as the B16F10 *in vivo* model, it may be necessary to release a responsible amount of LAPONITE® within a short period of time and then continue to release it. Taken together, these results clearly demonstrate that DOX-loaded 6NC25, as a vehicle for sustained and localized drug delivery, seems better to target subcutaneous malignant tumors than free DOX and DOX-6NC75.

4. Conclusions

Using gelatin and LAPONITE®, we fabricated injectable STBs to explore how varying the LAPONITE®/gelatin ratio in STBs could influence their rheological properties, capacity for DOX release, and cytotoxicity toward melanoma, both *in vitro* and *in vivo*. First, we showed that different compositions of gelatin/LAPONITE® can differentially regulate pH-responsive DOX release from STBs. In particular, we observed that 6NC25 showed higher pH-responsiveness compared to other conditions, resulting in the controlled and sustained release of DOX under acidic conditions, while systems outside the target region could be minimally affected. Examination of the injection force and the rheological properties of STBs verified that the better STB characteristics of 6NC25 allow for the fastest recovery and lowest strain at low and high levels of deformation compared to 6NC75. Analysis of *in vitro* cytotoxicity and *in vivo* antitumor assays revealed that DOX-6NC25 with better pH-responsiveness showed more efficient targeting of malignant melanoma skin cancers compared to DOX-6NC75 by inducing DOX-mediated cell death and restricting tumor growth. It may be possible that the release of ions ranging from Si to Mg may contribute to the promotion of angiogenesis. However, we acknowledge that further studies will be required to investigate the detailed effect of ion release from LAPONITE® on inducing angiogenesis because it lies outside of the scope of this study. This work suggests that the pH-responsiveness and rheological properties of gelatin/LAPONITE®-based STBs could be tuned by controlling their compositions of gelatin/LAPONITE®, which emphasizes the importance of tailored engineering of STBs, where a highly controlled and sustained release of therapeutic drugs is required.

Author contributions

J Lee: idea, writing paper, revision, and correction. Y Wang, C Xue, and Y Chen: idea and experiment. M Qu, J Thakor, X Zhou, NR Barros, N Falcone, and P Young: experiment. K Lee, Y Zhu, H-J Cho, W Sun, B Zhao, S Ahadian, V Jucaud, and MR Dokmeci: revision and correction. A Khademhosseini: idea, revision, and correction. H-J Kim: idea, experiment, writing paper, revision, and correction.

Conflicts of interest

Ali Khademhosseini recently launched a start-up (Obsidio, Inc.) based on a STB for biomedical applications.

Acknowledgements

The authors gratefully acknowledge funding from the National Institutes of Health (HL140951, HL137193, and CA233981).

References

1 C. D. Lindsay and S. C. Heilshorn, *Biofabrication and 3D Tissue Modeling*, 2019, vol. 3, p. 94.
2 C. Xue, H. Xie, J. Eichenbaum, Y. Chen, Y. Wang, F. W. van den Dolder, J. Lee, K. Lee, S. Zhang and W. Sun, *Biotechnol. J.*, 2020, **15**, 1900456.
3 R. K. Avery, H. Albadawi, M. Akbari, Y. S. Zhang, M. J. Duggan, D. V. Sahani, B. D. Olsen, A. Khademhosseini and R. Oklu, *Sci. Transl. Med.*, 2016, **8**, 365ra156–365ra156.
4 A. K. Gaharwar, R. K. Avery, A. Assmann, A. Paul, G. H. McKinley, A. Khademhosseini and B. D. Olsen, *ACS Nano*, 2014, **8**, 9833–9842.
5 Q. Liu, C. Zhan, A. Barhoumi, W. Wang, C. Santamaria, J. B. McAlvin and D. S. Kohane, *Adv. Mater.*, 2016, **28**, 6680–6686.
6 M. H. Chen, L. L. Wang, J. J. Chung, Y.-H. Kim, P. Atluri and J. A. Burdick, *ACS Biomater. Sci. Eng.*, 2017, **3**, 3146–3160.
7 J. F. Reuther, R. A. Scanga, A. Shahrokhinia and P. Biswas, in *Self-Healing Polymer-Based Systems*, Elsevier, 2020, pp. 293–367.
8 S. Samimi Gharaie, S. M. H. Dabiri and M. Akbari, *Polymer*, 2018, **10**, 1317.
9 A. Sheikhi, S. Afewerki, R. Oklu, A. K. Gaharwar and A. Khademhosseini, *Biomater. Sci.*, 2018, **6**, 2073–2083.
10 C. Li, C. Mu, W. Lin and T. Ngai, *ACS Appl. Mater. Interfaces*, 2015, **7**, 18732–18741.
11 E. Boedtkjer and S. F. Pedersen, *Annu. Rev. Physiol.*, 2020, **82**, 103–126.
12 G. Merlino, M. Herlyn, D. E. Fisher, B. C. Bastian, K. T. Flaherty, M. A. Davies, J. A. Wargo, C. Curiel-Lewandrowski, M. J. Weber and S. A. Leachman, *Pigm. Cell Melanoma Res.*, 2016, **29**, 404–416.
13 Y. Kato, S. Ozawa, C. Miyamoto, Y. Maehata, A. Suzuki, T. Maeda and Y. Baba, *Cancer Cell Int.*, 2013, **13**, 1–8.
14 L. Liu, W. Yao, Y. Rao, X. Lu and J. Gao, *Drug Delivery*, 2017, **24**, 569–581.
15 S. Wang, Y. Wu, R. Guo, Y. Huang, S. Wen, M. Shen, J. Wang and X. Shi, *Langmuir*, 2013, **29**, 5030–5036.
16 R. Salehi, E. Alizadeh, H. S. Kafil, A. M. Hassanzadeh and M. Mahkam, *RSC Adv.*, 2015, **5**, 105678–105691.

17 L. J. Villarreal-Gomez, A. Serrano-Medina, E. J. Torres-Martinez, G. L. Perez-Gonzalez and J. M. Cornejo-Bravo, *e-Polym.*, 2018, **18**, 359–372.
18 P. Priya, R. M. Raj, V. Vasanthakumar and V. Raj, *Arabian J. Chem.*, 2020, **13**, 694–708.
19 S. Mangalathillam, N. S. Rejinold, A. Nair, V.-K. Lakshmanan, S. V. Naira and R. Jayakumar, *Nanoscale*, 2012, **4**, 239.
20 P. Sahu, S. K. Kashaw, S. Sau, V. Kushwah, S. Jain, R. K. Agrawal and A. K. Iye, *Colloids Surf., B*, 2019, **174**, 232–245.
21 M. Sabitha, N. S. Rejinold, A. Nair, V.-K. Lakshmanan, S. V. Nair and R. Jayakuma, *Carbohydr. Polym.*, 2013, **91**, 48–57.
22 T. N. Chinembiri, M. Gerber, L. du Plessis, J. du Preez and J. du Plessis, *AAPS PharmSciTech*, 2015, **16**, 1390–1399.
23 M. A. Khan, J. Pandit, Y. Sultana, S. Sultana, A. Ali, M. Aqil and M. Chauhan, *Drug Delivery*, 2015, **22**, 795–802.
24 S. E. Kudaibergenov, *Polym. Adv. Technol.*, 2021, **32**, 906–918.
25 T. Coradin, S. Bah and J. Livage, *Colloids Surf., B*, 2004, **35**, 53–58.